

Optimization of mixing time in a ladle with dual plugs

Dian-qiao Geng, Hong Lei, and Ji-cheng He

Key Laboratory of Electromagnetic Processing of Materials (Ministry of Education of China), Northeastern University, Shenyang 110819, China
(Received: 25 January 2010; revised: 11 February 2010; accepted: 7 February 2010)

Abstract: Based on the two-phase fluid (Eulerian-Eulerian) model, a mathematical model about the gas-liquid flow and mixing behavior was developed to investigate the effect of the offset of dual plugs, the included angle of dual plugs with a center point, and gas flow rate on the mixing time in a ladle with dual plugs. Numerical results indicate that two types of recirculation zones exist in the ladle. One is the middle recirculation between gas and liquid plumes, and the other is the sidewall recirculation between plumes and the ladle sidewall. The correction shows that the mixing time is in proportion to -0.2676 power of gas flow rate. There is a unique optimum offset of dual plugs with a particular included angle, in turn, a unique optimum included angle of dual plugs exists with a particular offset.

Keywords: ladles; refining; mixing time; optimization; numerical simulation

[This work was financially supported by the National High-tech Research and Development Program of China (No.2009AA03Z530), the National Natural Science Foundation of China and Shanghai Baosteel (No.50834010), and the Key Project of the Ministry of Education of China (No.108036).]

1. Introduction

Recently, with increasing demands for high-quality steel, secondary refining in gas stirred ladles plays a significant role in the modern steel industry. The efficiency of metallurgical reactions, such as degassing, deoxidation, and desulphurization, in gas stirred ladles is basically related to mixing phenomena. Moreover, the homogeneity of temperature or chemical composition is also concerned with mixing phenomena in gas stirred ladles. Therefore, the study of mixing phenomena in gas stirred ladles has received considerable attention over the years [1-7]. Usually, the mixing degree in gas stirred ladles can be evaluated from a degree of 95% mixing time, which is defined as the maximum time for the concentration of all monitoring points to fall within a 5% deviation of the homogeneous value. According to the previous study, the shortest mixing time can be obtained in the case of single-plug placed off-center [3]. However, since the slag entrapment is one of the main sources of inclusions in steel [8], metallurgical reactions, such as deoxidation and

alloy homogenization, requires gentle mixing at the metal-slag interface and maintenance of an unbroken slag layer. Thus, a ladle stirred with dual plugs was developed. In addition, lots of studies have been proposed in view of ladles with dual plugs [2-6]. As shown in Fig. 1, the position of dual plugs can be determined with offset (L) and included angle (θ). As one would note here, although the effect of offset and included angle on the mixing time has been studied, not much detailed information about the effect of included angle is available in these researches. The quasi-single phase model derived for an axisymmetrical gas stirred ladle with a centrally placed plug was still employed in some studies [3-4]. Obviously, the quasi-single phase model cannot be very accurate to study transport phenomena in a ladle with dual plugs. Thus, the purpose of the present work was to optimize the location of dual plugs, which could yield the minimum mixing time, and to develop a new correlation for the mixing time based on a wide variation of location parameters (L/R , θ) and gas flow rate (Q_g), as shown in Table 1 (R is the radius of the ladle bottom).

Corresponding author: Dian-qiao Geng E-mail: gengdianqiao@163.com

© University of Science and Technology Beijing and Springer-Verlag Berlin Heidelberg 2010

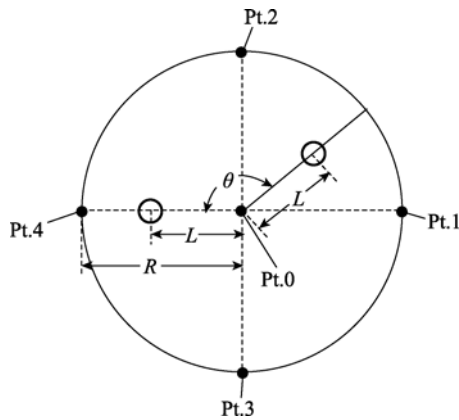


Fig.1. Schematic diagram of dual plugs at the ladle bottom.

Table 1. Parameters of the ladle with dual plugs

Parameter	Value
L/R	0.25, 0.33, 0.5, 0.75, and 0.80
θ	$\pi/2, 2\pi/3, 5\pi/6, \text{ and } \pi$
$Q_g / (\text{NL}\cdot\text{min}^{-1})$	200, 300, 400, and 500

2. Mathematical model

2.1. Assumptions

The mathematical model for fluid flow and tracer transportation was based on the following assumptions.

(a) The fluids in both gas and liquid phases were Newtonian, viscous and incompressible, and the fluid flow was at the steady state.

(b) The effect of top slag on the fluid flow was neglected and the free surface in the ladle was assumed to be flat.

(c) The deformation of gas bubbles was not taken into account, so the gas bubbles were assumed to be spherical, and their interactions leading to coalescence and breakup were neglected.

(d) The fluid flow in the ladle was assumed to be an isothermal process.

2.2. Governing equations

The multiphase flow in a gas-stirred ladle was simulated by the Eulerian-Eulerian model. The continuity and momentum conservation equations for the k -th phase are shown as follows [9-10].

(1) Continuity equation:

$$\nabla \cdot (\alpha_k \rho_k \vec{u}_k) = 0 \quad (1)$$

(2) Momentum conservation equation:

$$\begin{aligned} \nabla \cdot (\alpha_k \rho_k \vec{u}_k \vec{u}_k) &= -\alpha_k \nabla p + \vec{F}_{\text{drag},k} + \alpha_k \rho_k \vec{g} + \\ \nabla \cdot [\alpha_k \mu_{\text{eff}} \rho_k (\nabla \vec{u}_k + (\nabla \vec{u}_k)^T)] & \end{aligned} \quad (2)$$

where $k=1$ or 2 denotes the gas and liquid phases, respectively, ρ_k the density of the k -th phase, \vec{u}_k the velocity vector of the k -th phase, p is the pressure, μ_{eff} is the effective viscosity and can be determined by the standard κ - ε turbulence model. Because the whole space domain is shared by the two phases, the sum of both volume fractions should be equal to one, *i.e.*, $\alpha_1 + \alpha_2 = 1$. $\vec{F}_{\text{drag},k}$ is the drag force between two phases and can be expressed as

$$\vec{F}_{\text{drag},l} = -\vec{F}_{\text{drag},g} = \frac{3}{4} \frac{C_D}{d_b} \alpha_g \rho_l |\vec{u}_g - \vec{u}_l| (\vec{u}_g - \vec{u}_l) \quad (3)$$

with

$$C_D = \max \left[\frac{24}{Re_b} (1 + 0.15 Re_b^{0.687}), 0.44 \right] \quad (4)$$

and

$$Re_b = \frac{\rho_l |\vec{u}_g - \vec{u}_l| d_b}{\mu_l} \quad (5)$$

where C_D is the drag coefficient [11], Re_b the bubble Reynolds number, d_b the bubble diameter and can be expressed as [12]

$$d_b = 0.091 \left(\frac{\sigma}{\rho_l} \right)^{0.5} \left(\frac{2Q_g}{\pi d_o^2} \right)^{0.44} \quad (6)$$

where σ is the surface tension and d_o the diameter of the nozzle exit.

(3) Tracer transport equation [13-14]:

$$\frac{\partial(\rho_l C)}{\partial t} + \nabla \cdot (\rho_l \vec{u}_l C) = \nabla \cdot \left[\frac{\mu_{\text{eff}}}{Sc} (\nabla C) \right] \quad (7)$$

where C is the tracer dimensionless concentration and Sc the turbulent Schmidt number. The mixing time (τ_{mix}) was defined as the time required to obtain a 95% level of homogeneity, *i.e.*, the concentrations of all points in the bath were within $\pm 5\%$ deviation of the homogeneous concentration value.

2.3. Boundary conditions and solution method

For the refractory walls in the ladle, no-slip wall boundary conditions were applied. For the free surface, the sym-

metry boundary condition was imposed. Furthermore, gas bubbles reaching the free surface were assumed to escape at their flotation velocity.

The finite volume method was used to solve the governing differential equations [15]. The computational fluid dynamics Package, CFX 5.7, was employed to perform the calculation. Moreover, the grids consisted of about 900000 control volumes. The convergence criteria was that the value of the root mean square normalized residual for variables was less than 1×10^{-5} and the global imbalances, which means the ratios of the difference between the total input mass flux and the total output mass flux to the total input mass flux, was less than 0.1%. The geometrical parameters of the ladle and the material properties in the calculation are shown in Table 2.

Table 2. Calculation parameters

Parameter	Value
Up diameter of ladle / m	4.0
Down diameter of ladle / m	3.6
Height of ladle / m	3.7
Density of argon gas (STP) / ($\text{kg}\cdot\text{m}^{-3}$)	1.28
Density of liquid steel / ($\text{kg}\cdot\text{m}^{-3}$)	7020
Viscosity of liquid steel / (Pa·s)	0.0061

2.4. Tracer addition position and monitoring points

Fig. 2 shows the effect of the tracer addition position at the free surface on mixing time. The offset of the tracer addition points in the right direction has a more profound effect on the mixing time than that in the front direction. In addition, the mixing is the most effective, while the tracer was added at the middle point of dual plugs. Therefore, such

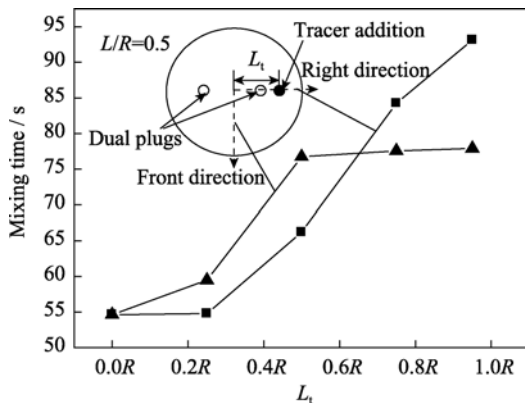


Fig. 2. Variation of mixing time under different tracer addition points.

a tracer addition point is adopted in the numerical experiments. It has been reported that the junction of the vertical sidewall and the base of the ladle is the relatively slowly mixing region [3-4]. Furthermore, stagnant flow can also be observed in the bottom centre [4]. Therefore, as shown in Fig. 1, four monitoring points (Pt1-Pt4) are placed around the junction of the vertical sidewall, and the base of the ladle while a monitoring point (Pt.0) is placed at the center between dual plugs on the bottom.

3. Results and discussion

3.1. Validity of the model

Fig. 3 shows that the mixing time decreases with increasing gas flow rate, and the predicted mixing time agrees well with the experimental data [3]. The difference between the numerical results and the experimental data comes from the introduction of the conductivity probe because such a direct measure method can change the flow field in the ladle.

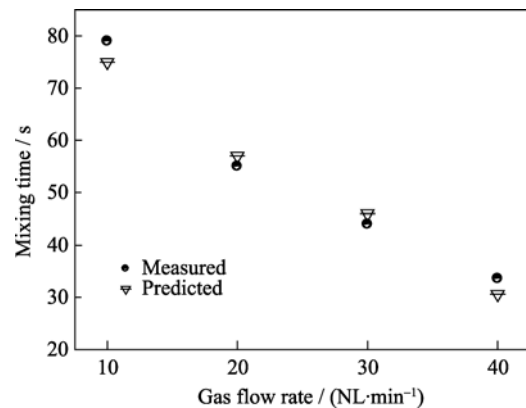


Fig. 3. Comparison of calculated mixing time with the experimental values [3].

3.2. Fluid flow in the ladle

Fig. 4 shows the typical flow patterns in the ladle with dual plugs, which were placed diametrically and were opposed at half radius. The gas flow rate is 300 NL/min. The upstream jets due to gas injections from the dual plugs form two plumes and expands as they rises. Then, the plumes split into two main streams and flow down along with the sidewall. Fig. 4 also shows that there are two types of recirculation in the ladle. One is the middle recirculation between two plumes, while another is the sidewall recirculation between the plume and the sidewall. The liquid lateral flow displaces the plume, and bubbles rise along the curved trajectories. Therefore, the plume bending phenomenon

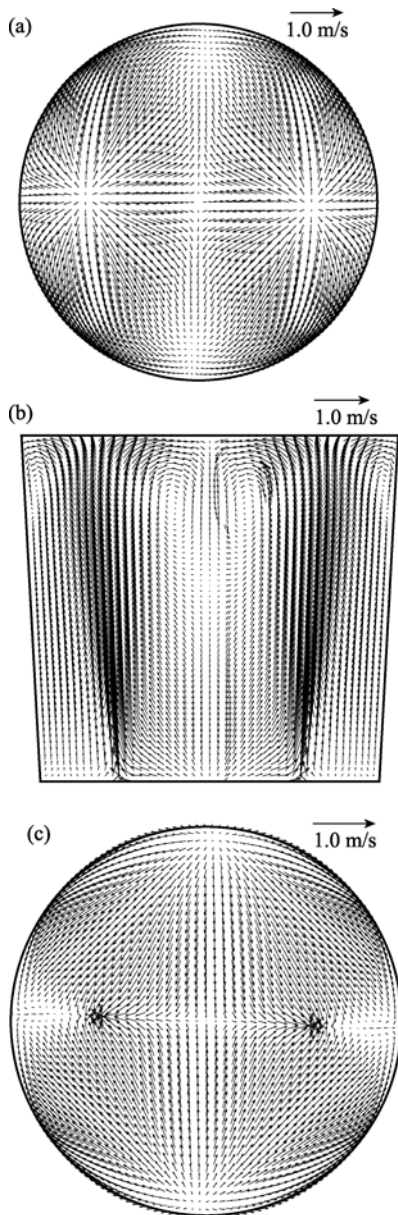


Fig. 4. Predicted flow patterns in the ladle with dual plugs: (a) top of the ladle; (b) main section; (c) bottom of the ladle.

appears in Fig. 4. Such an interesting phenomenon has also been observed in the water model of the ladle with dual plugs [16].

3.3. Effect of the offset and included angle of dual plugs

The strength and size of the recirculation are two key factors to affect the mixing process in the ladle. With increasing distance between dual plugs, the middle recirculation becomes larger, but the side recirculation becomes smaller. On the other hand, the distance between dual plugs is determined by the offset and the included angle of dual

plugs with a center point. Therefore, the effect of the offset and the included angle of dual plugs with a center point on the mixing time are discussed in the present context. Fig. 5 shows the dependence of mixing time and the offset of dual plugs. Fig. 5(a) shows that the mixing time increases with increasing offset when the included angle is $\pi/2$. Two reasons lead to this phenomenon. First the dual plugs are very close to each other. Therefore, the sidewall recirculation plays a key role on stirring. Second, with increasing offset,

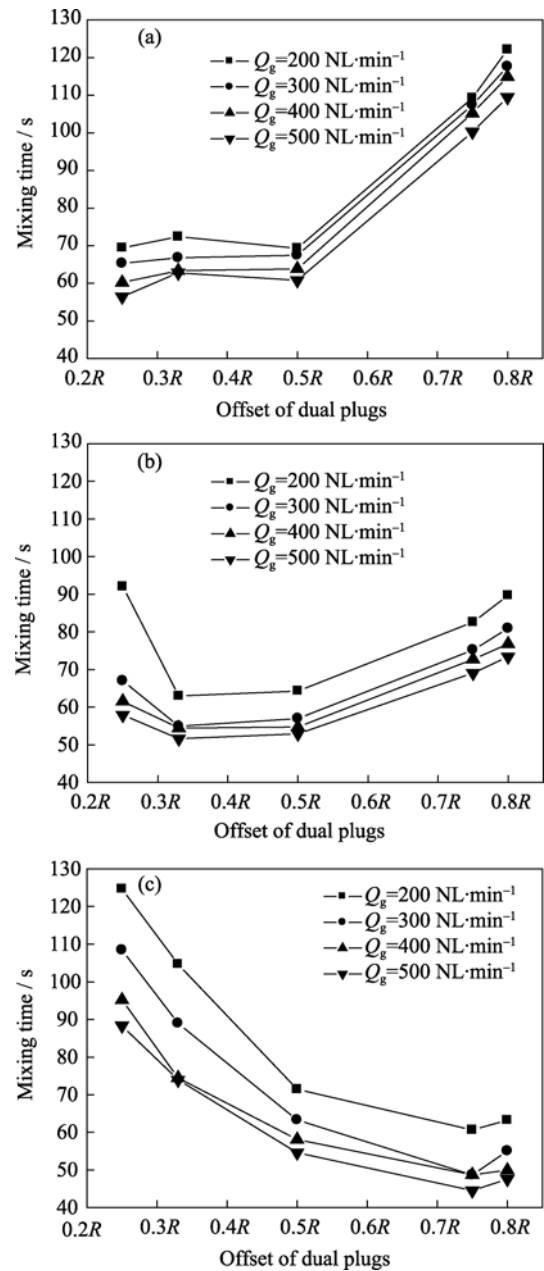


Fig. 5. Variation of mixing time with the offset of dual plugs at different included angles: (a) $\theta = \pi/2$; (b) $\theta = 2/3\pi$; (c) $\theta = \pi$.

the smaller sidewall recirculation results in a weaker stirring effect. Fig. 5(c) shows that in the case of $\theta=\pi$, the mixing time decreases as the offset increases to $0.75R$ and then has a tendency to increase because the mixing time is more dependent on the middle recirculation than the sidewall recirculation with further increasing offset. Moreover, when the offset increases to $0.8R$, the sidewall recirculation almost disappears. Therefore, the dead zone becomes larger, and this prolongs the mixing time. Fig. 5(b) shows that the mixing time decreases as the offset is up to $0.33R$ and then increases with increasing offset. The major reason is that the stirring effect of the middle recirculation becomes more important in the case of $\theta=2/3\pi$. Although the stirring effect of the sidewall recirculation is weakened by increasing the offset, the stirring effect of the middle recirculation is enhanced simultaneously.

Fig. 6 shows the effect of the included angle of dual plugs with a center point on the mixing time. The sidewall recirculation turns to be more important than the middle recirculation in the case of $L=0.25R$. Therefore, Fig. 6(a) shows that the mixing time increases with the included angle increasing first and then decreases. However, a completely adverse response of mixing time with the included angle can be observed in Fig. 6(b) when the offset of dual plugs increases from $0.25R$ to $0.5R$. The mixing time decreases with the increasing included angle of dual plugs. Then, the mixing time increases after at $5/6\pi$ of the included angle. Fig. 6(c) shows the mixing time decreases with increasing included angle, and the optimum included angle is π . The major reason is that the middle recirculation turns to be more important with the increasing offset of dual plugs.

3.4. Correlation for mixing time

As shown in Figs. 5 and 6, neither the relationship between mixing time and offset nor that between mixing time and included angle is monotonic. In other words, the effect of offset and included angle on mixing time should be interactive. Therefore, this multiplex effect should be taken into account in correlation. The correlation for mixing time is shown as follows:

$$\tau_{\text{mix}} = 9.448 \times 10^{-5} \left(\frac{L}{R}\right)^{-2.1315} \times \theta^{-8.15} \left(\frac{L}{R} + 2.617\theta\right)^{10.195} Q_g^{-0.2676} \quad (8)$$

As shown in Fig. 7, the differences between the devel-

oped correction of simulated mixing time and actual values are various within +14.3% and -16.9%. In addition, the mixing time decreases in proportion to 0.2676 power of gas flow rate, which is relatively smaller than that in the previous study derived from water modeling [5]. The term of $\left(\frac{L}{R} + 2.617\theta\right)^{10.195}$ indicated that the mixing time has a complicated relationship with the offset and the included angle of dual plugs with a center point.

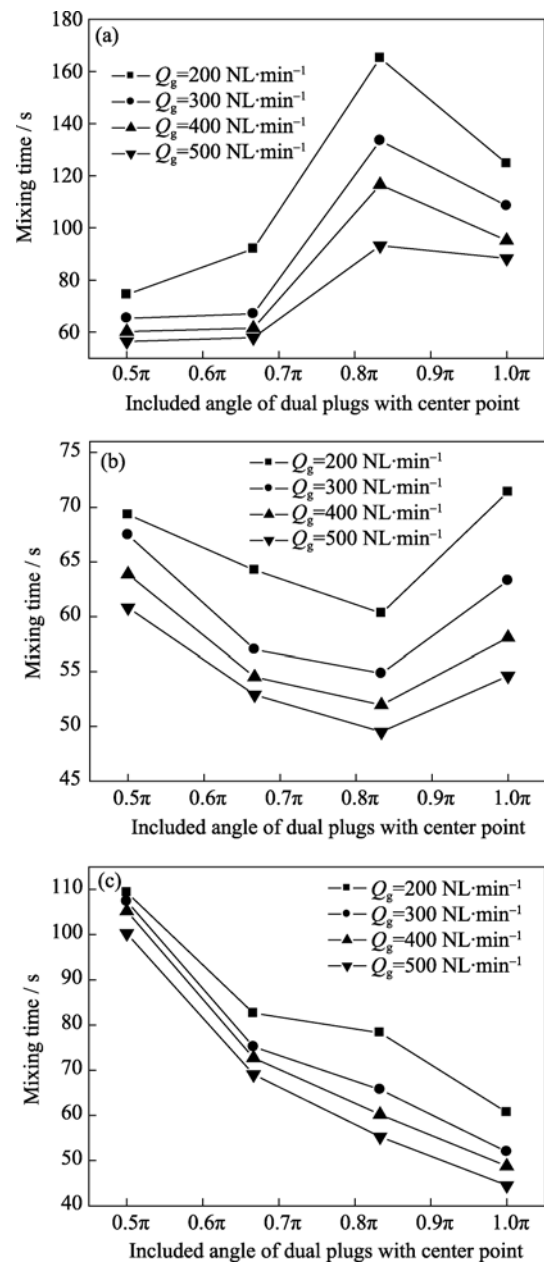


Fig. 6. Variation of mixing time with the included angle of dual plugs with a center point: (a) $L=0.25R$; (b) $L=0.5R$; (c) $L=0.75R$.

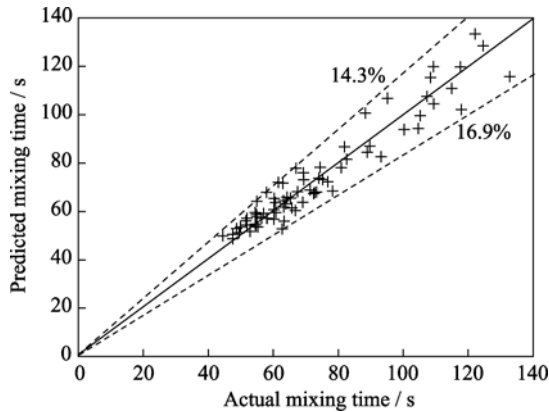


Fig. 7. Predicted mixing time vs. actual values.

4. Conclusions

(1) There are two types of recirculation zones in the ladle. One is the middle recirculation between two plumes, and the other is the sidewall recirculation between the plume and the sidewall.

(2) The mixing time had a complicated relationship with the offset and the included angle of dual plugs with a center point: there is a unique optimum offset of dual plugs with a particular included angle, while there was a unique optimum included angle of dual plugs with a particular offset.

(3) A correction for mixing time in the ladle with dual plugs is expressed as $\tau_{\text{mix}} = 9.448 \times 10^{-5} \left(\frac{L}{R} \right)^{-2.1315} \times \theta^{-8.15} \left(\frac{L}{R} + 2.617\theta \right)^{10.195} Q_g^{-0.2676}$.

References

- [1] M. Warzecha, J. Jowza, P. Warzecha, and H. Pfeifer. Numerical and experimental investigations of steel mixing time in a 130-t ladle, *Steel Res. Int.*, 79(2008), No.11, p.852.
- [2] D. Mazumdar and J. W. Evans, Macroscopic models for gas stirred ladles, *ISIJ Int.*, 44(2004), No.3, p.447.
- [3] S. Joo and R.I.L. Guthrie, Modeling flows and mixing in steelmaking ladles designed for single- and dual-plug bubbling operations, *Metall. Mater. Trans. B*, 23(1992), No.6, p.765.
- [4] M.Y. Zhu, T. Inomoto, I. Sawada, and T.C. Hsiao, Fluid flow and mixing phenomena in the ladle stirred by argon through multi-tuyere, *ISIJ Int.*, 35(1995), No.5, p.472.
- [5] J. Mandal, S. Patil, M. Madan, and D. Mazumdar, Mixing time and correlation for ladles stirred with dual porous plugs, *Metall. Mater. Trans. B*, 36(2005), No.4, p.479.
- [6] M. Madan, D. Satish, and D. Mazumdar. Modeling of mixing in ladles fitted with dual plugs, *ISIJ Int.*, 45(2005), No.5, p.677.
- [7] H.Y. Tang, J.S. Li, C. H. Xie, S.F. Yang, K.M. Sun, and D.S. Wen, Rational argon stirring for a 150-t ladle furnace, *Int. J. Miner. Metall. Mater.*, 16(2009), No.4, p.383.
- [8] L. Zhang and B.G. Thomas, State of the art in evaluation and control of steel cleanliness, *ISIJ Int.*, 43(2003), No.3, p.271.
- [9] J.H. Wei and H T. Hu, Mathematical modelling of molten steel flow process in a whole RH degasser during the vacuum circulation refining process: Mathematical model of the flow, *Steel Res. Int.*, 77(2006), No.1, p.32.
- [10] H. Turkoglu and B. Farouk, Mixing time and liquid circulation rate in steelmaking ladles with vertical gas injection, *ISIJ Int.*, 31(1991), No.12, p.1371.
- [11] P. Chen, J. Sanyal, and M.P. Dudukovic, CFD modeling of bubble columns flows: implementation of population balance, *Chem. Eng. Sci.*, 59(2004), No.22, p.5201.
- [12] M. Sano and K. Mori, Size of bubbles in energetic gas injection into liquid metal, *Trans. Iron Steel Inst. Jpn.*, 20(1980), No.10, p.675.
- [13] S.K. Ajmani, Dash, S. Chandra, and C. Bhanu. Mixing evaluation in the RH process using mathematical modelling, *ISIJ Int.*, 44(2004), No.1, p.82.
- [14] F. Ahrenhold and W. Pluschkell, Mixing phenomena inside the ladle during RH decarburization of steel melts, *Steel Res. Int.*, 70(1999), No.8, p.314.
- [15] S.V. Patankar and D.B. Spalding, A calculation procedure for heat, mass and momentum transfer in three-dimensional parabolic flows, *Int. J. Heat Mass Transfer*, 15(1972), No.10, p.1787.
- [16] D. Guo and G.A. Irons, Modeling of gas-liquid reactions in ladle metallurgy: Part I. Physical Modeling, *Metall. Mater. Trans. B*, 31(2000), No.6, p.1447.